

Cite this: *Green Chem.*, 2025, 27, 1348

Received 4th November 2024,

Accepted 7th January 2025

DOI: 10.1039/d4gc05617e

rsc.li/greenchem

Highly efficient synthesis of *tert*-butyl esters using (Boc)₂O under solvent/base-free electromagnetic milling conditions: a new reaction model†

Yunxia Liu,^a Yan Zhang,^a Yingyu Qu,^a Qing Liu,^a Kai Cao,^{*b} Fachao Yan,^a Lizhi Zhang,^a Xinjin Li,^{id} ^{*a} Zengdian Zhao^{*a} and Hui Liu^{id} ^{*a}

A novel and efficient method has been developed for the synthesis of *tert*-butyl esters using (Boc)₂O as the *tert*-butyl source, facilitated by electromagnetic milling. This green and sustainable approach is solvent-free, base-free, and operates without the need for additional heating, making it highly appealing for eco-friendly synthesis. The entirely neutral reaction environment proves particularly advantageous for synthesizing or modifying sensitive drug

molecules, especially in late-stage functionalization. In this process, ferromagnetic rods, used as grinding media, become magnetized and charged under a high-speed rotating magnetic field. This magnetization plays a crucial role in bond activation by coordinating with the charged ferromagnetic rods, introducing a novel mechanism for bond activation that could inspire further research in this emerging field.

Green foundation

1. This work introduces a novel and efficient method for the synthesis of *tert*-butyl esters using (Boc)₂O as the *tert*-butyl source, facilitated by electromagnetic milling.
2. This solvent-free, base-free, and heating-free approach presents an attractive, green, and sustainable pathway. The neutral reaction environment is especially beneficial for the late-stage modification of sensitive drugs in drug discovery, ensuring both efficiency and compatibility with delicate compounds.
3. In this process, ferromagnetic rods, acting as grinding media, become magnetized and charged under a high-speed rotating magnetic field. The magnetization is key to bond activation, as it interacts with the charged rods, introducing a novel mechanism that could inspire further research in this emerging field.

Introduction

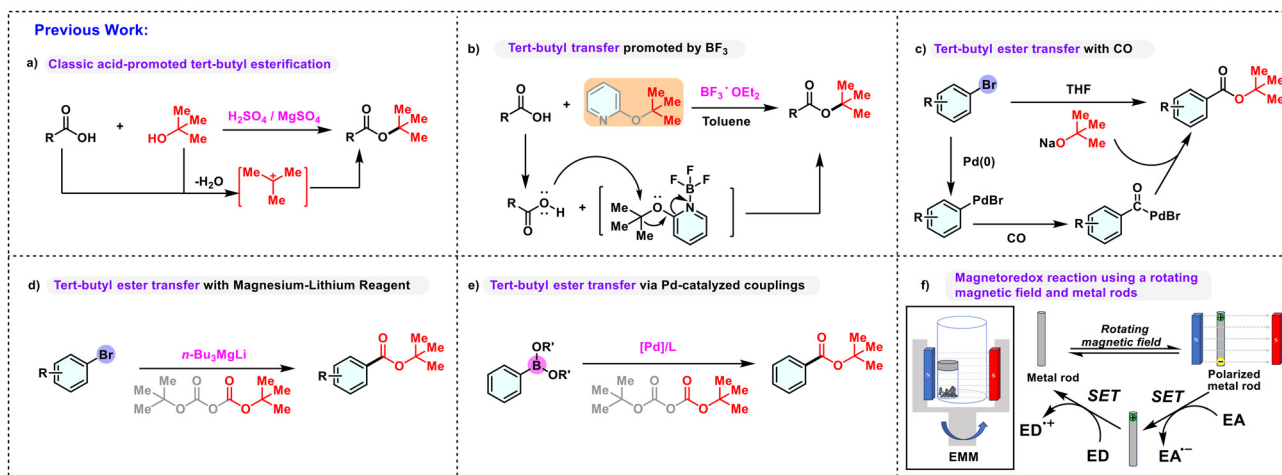
tert-Butyl is a crucial functional group in organic synthesis, known for its substantial steric hindrance and pronounced spatial effects in reactions. It acts as a large steric group, providing kinetic stability and resisting nucleophilic attacks, which make it an important protective group for carboxylic acids.¹ Its utility is especially notable in the synthesis of bioactive compounds like hepatitis C virus NS3 protease inhibitors² and GABA-T inhibitors.³ Various methods for synthesizing

tert-butyl esters have been developed. One of the earliest synthetic methods for preparing *tert*-butyl esters is the Fischer–Speier esterification, developed in 1895. This method involves the reaction of carboxylic acids with *tert*-butanol under the catalysis of acids, typically either Lewis acids or Brønsted acids (Scheme 1a).⁴ It lays the foundation for the development of other *tert*-butyl esterification methods and remains a classic technique in organic chemistry. Later, Wright and co-workers introduced a method for *tert*-butyl ester synthesis using sulfuric acid and an excess of *tert*-butyl alcohol in the presence of anhydrous magnesium sulfate.⁵ This modification enhanced the reaction efficiency and broadened the scope of applicable substrates, offering an alternative to the Fischer–Speier esterification for preparing *tert*-butyl esters under different conditions. In 2018, La *et al.* introduced a BF₃·OEt₂-promoted *tert*-butyl esterification process, employing 2-*tert*-butylpyridine as an innovative *tert*-butyl surrogate⁶ (Scheme 1b). This method enables a more controlled esterifi-

^aSchool of Chemistry and Chemical Engineering, Shandong University of Technology, Zibo, Shandong 255049, China. E-mail: huiliu1030@163.com, zhaozengdian@sdut.edu.cn, lixj@sdut.edu.cn

^bPharmacy Department, Zibo Central Hospital, Zibo 255036, China. E-mail: wwwcaokai@126.com

† Electronic supplementary information (ESI) available. See DOI: <https://doi.org/10.1039/d4gc05617e>



Scheme 1 Research on the synthesis of *tert*-butyl esters (EA – electron acceptor; ED – electron donor; EMM – electromagnetic milling).

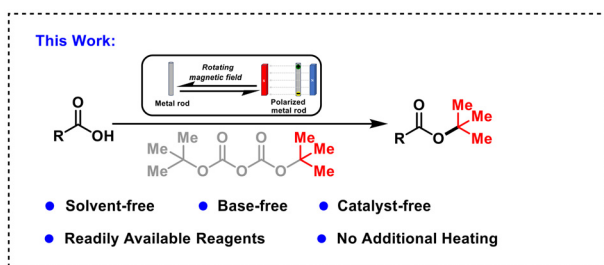
cation process, overcoming the limitation of using strong concentrated acids, which can influence the esterification of substrates bearing acid-sensitive functional groups. Meanwhile, Skrydstrup *et al.* developed a palladium-catalyzed *tert*-butyloxy-carbonylation reaction of aryl bromides with carbon monoxide, offering a more direct route to *tert*-butyl esters⁷ (Scheme 1c). However, despite the efficiency of this process, the use of toxic carbon monoxide posed a significant limitation, highlighting the need for safer alternatives in synthetic methodologies.

In contrast, di-*tert*-butyl dicarbonate ((Boc)₂O), a safer, more cost-effective, and efficient amino acid protectant, has become widely utilized across several industries, including pharmaceuticals, protein and peptide synthesis, biochemical food production, and cosmetics.⁸ Due to its broad applicability and ease of use, (Boc)₂O has also proven instrumental in the synthesis of *tert*-butyl esters, offering a safer alternative to methods involving more hazardous reagents, such as carbon monoxide, and reinforcing its importance in modern synthetic chemistry. In 2008, Balsells and colleagues introduced a method for preparing *tert*-butyl esters at low temperatures by reacting aryl bromides with a magnesium–lithium reagent and (Boc)₂O, as shown in Scheme 1d.⁹ Later, in 2014, Li *et al.* successfully developed a palladium-catalyzed synthesis process of *tert*-butyl esters using boric acid or boronic acid esters in combination with (Boc)₂O (Scheme 1e).¹⁰ These methods offer efficient routes for *tert*-butyl ester formation under mild conditions. However, the highly moisture and air sensitive metallic reagent and expensive palladium catalyst limited their application.

Therefore, developing a green and efficient method for synthesizing *tert*-butyl ester compounds under mild reaction conditions presents a significant challenge. In recent years, the field of mechanochemistry has experienced significant advancements, yielding numerous pivotal research findings, such as those by Ito (redox reactions of small organic molecules using ball milling and piezoelectric materials and solid-

state cross-coupling of insoluble aryl halides),¹¹ Bolm (the first to perform asymmetric organocatalysis in a ball mill),¹² Friščić (constructing porous MOFs using LAG and ILAGs),¹³ Pilarski (solvent-free catalytic C–H and C–X functionalization without a ball mill),¹⁴ Borchardt (photo- or thermo-mechanochemistry),¹⁵ Gouverneur (fluorochemicals from fluorspar *via* a phosphate-enabled mechanochemical process that bypasses HF),¹⁶ Browne (the use of temperature-controlled mechanochemistry to enable mechanochemical nickel-catalyzed Suzuki–Miyaura couplings),¹⁷ Wang (covalent and non-covalent functionalization of fullerenes and related materials through mechanochemistry),¹⁸ Lian (new reactions with ball milling and piezoelectric materials),¹⁹ Wei (mechanochemical synthesis of *α*-halo alkylboronic esters),²⁰ Zhang and Szostak (the first mechanochemical decarbonylative coupling),²¹ and Yu and Su (*α*-C–H functionalization of glycine derivatives under mechanochemically accelerated aging en route to the synthesis of 1,4-dihydropyridines and *α*-substituted glycine esters).²² Recently, our group has developed a novel multi-energy field coupling apparatus for boronization, Suzuki coupling, and cyanidation in a solvent-free system.²³ Electromagnetic milling (EMM) represents an innovative grinding device that utilizes small ferromagnetic particles as the grinding media within a rotating electromagnetic field.²⁴ The EMM consists of an inductor that generates a rotating magnetic field, positioned within a stationary housing that serves as the working chamber. Unlike traditional ball mills, where the housing rotates, the EMM features a stationary housing, while the ferromagnetic rods within the working chamber are set into motion by the vortex electromagnetic field. This motion enhances the mixing of solid reactants and increases the surface area through high-speed collisions of the ferromagnetic rods, leading to improved reaction efficiency compared to conventional ball mills.

Very recently, we discovered that this EMM device can facilitate redox reactions in organic molecules by transferring a single electron between ferromagnetic rods and organic mole-



Scheme 2 Highly efficient synthesis of *tert*-butyl esters using $(\text{Boc})_2\text{O}$ under solvent/base-free electromagnetic milling conditions.

cules²⁵ (Scheme 1f). On the basis of these results, we designed a method to generate a *tert*-butyl radical from $(\text{Boc})_2\text{O}$ via a single electron transfer process under electromagnetic milling conditions, efficiently synthesizing *tert*-butyl esters with aromatic carboxylic acids (Scheme 2).

Results and discussion

We began the optimization by using *p*-methoxybenzoic acid as a template substrate for the synthesis of *tert*-butyl esters. Initially, we explored the effects of ferromagnetic rods on the reaction efficacy. The results revealed that variations in rod specifications had a mild effect on the reaction efficiency (see Fig. 1A). Notably, when using ferromagnetic rods with dimen-

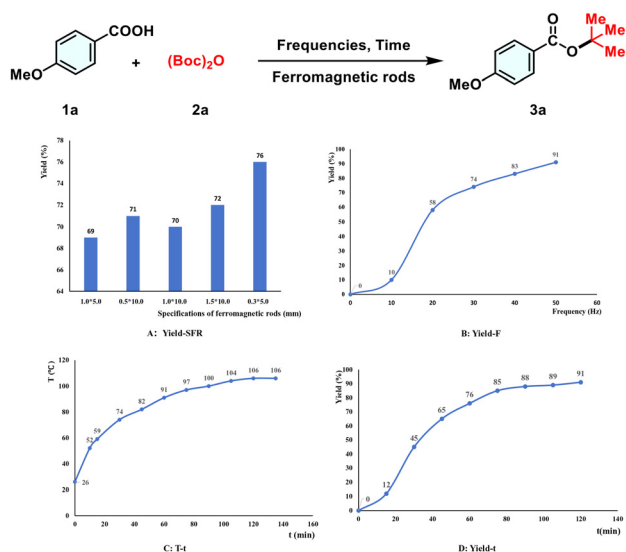


Fig. 1 Optimization of the synthesis conditions of *tert*-butyl esters under electromagnetic milling conditions. Conditions: **1a**: 0.5 mmol, **2a**: 1.0 mmol, high temperature and pressure resistant reaction tube: 10 mL, ferromagnetic rods: SUS304, 5 g. (A) The influence of different specifications of ferromagnetic rods on the reaction yield (SFR: specifications of ferromagnetic rods, frequency: 50 Hz, reaction time: 1 h). (B) Yields at different frequencies (F: frequency, ferromagnetic rods: 0.3 × 5.0 mm, reaction time: 2 h). (C) Temperature for different time periods (ferromagnetic rods: 0.3 × 5.0 mm, frequency: 50 Hz). (D) Yields for different time periods (ferromagnetic rods: 0.3 × 5.0 mm, frequency: 50 Hz).

sions of 1.0 × 30.0 mm or 1.0 × 50.0 mm, no target product was obtained, regardless of solvent presence (see Fig. S7†). However, a rod dimension of 0.3 × 5.0 mm resulted in a 76% yield, prompting us to select this specification for further investigation.

We speculated that smaller steel needle diameters would result in a greater number of effective collisions. As the reaction progressed, the yield steadily increased, ultimately reaching 91% after 2 hours.

To further explore the scope of the reactions, we investigated various aromatic and alkyl carboxylic acids under the optimized conditions. The results revealed that both electron-rich and electron-deficient carboxylic acids can be efficiently converted into *tert*-butyl ester products. However, electron-rich carboxylic acids (**3a**, **3b** and **3c**) exhibited a higher conversion rate, while benzoic acid (**3d**) and electron-withdrawing carboxylic acids (**3e** and **3f**) were less efficient. Notably, carboxylic acids containing halogen atoms (**3g**, **3h** and **3i**) produced the corresponding products in yields of 62%, 75% and 49%, respectively. It is important to highlight that the 62% yield with *p*-fluorobenzoic acid (**3g**) is likely due to the low boiling point of its product, leading to more significant losses during the collection process.

When the functional group on benzoic acid shifted to the *ortho*-position (**3j** and **3k**), the yield decreased somewhat due to steric hindrance. However, when the functional group was located at the *meta*-position relative to the carboxyl group, steric hindrance had little effect on the yield, resulting in moderate to excellent yields (**3l** and **3m**). Similarly, compound **3n** was obtained with a lower yield (36%) due to significant steric hindrance. Polycyclic compounds such as 2-naphthoic acid and 9-anthracene carboxylic acid were also successfully *tert*-butyl esterified. The esterification of 2-naphthoic acid was particularly efficient, achieving a yield of 83% (**3o**). In contrast, 9-anthracene carboxylic acid produced the target product (**3p**) at a lower yield, again due to steric hindrance. Furthermore, this method has been successfully applied to heterocyclic carboxylic acids, including pyridine (**3q**), thiophene (**3r** and **3s**), and indole (**3t**), resulting in excellent *tert*-butyl ester yields.

Additionally, cinnamic acids were efficiently converted into *tert*-butyl esters (**3u** and **3v**) under the standard conditions, achieving remarkable yields. Similarly, (*E*)-3-(thiophen-2-yl) acrylic acid was converted with a 65% yield (**3w**). Surprisingly, alkyl *tert*-butyl esters (**3x**, **3y**, **3z** and **3aa**) can also be synthesized from alkyl carboxylic acids and $(\text{Boc})_2\text{O}$ under optimal conditions. Notably, long-chain alkyl carboxylic acids, such as oleic acid, underwent *tert*-butyl esterification with an impressive yield of 85% (**3ab**). Furthermore, replacing $(\text{Boc})_2\text{O}$ with dimethyl di-carbonate for the methylation of carboxylic acids, whether aromatic, heteroaromatic, cinnamic, or alkyl, resulted in favorable conversions, yielding moderate to excellent results (**4a–4f**).

To evaluate the efficacy of this synthetic approach, a variety of complex bioactive compounds were employed in the synthesis of *tert*-butyl esters. Under the described reaction conditions, the desired *tert*-butyl esters were successfully obtained.

As illustrated in Table 1, the bioactive pharmaceutical agents include nonsteroidal anti-inflammatory drugs such as indomethacin (**1ac**), ketoprofen (**1ad**), and oxaprozin (**1ae**), all known for their antipyretic and analgesic properties, as well as februxostat (**1af**), which is recognized for its anti-gout effects.

To investigate the impact of electromagnetic milling (EMM) on the synthesis of *tert*-butyl esters, we conducted several control experiments under ball milling and solvent-based conditions using traditional magnetic stirring (Table 2). Under EMM conditions, **3a** was separated with a yield of 91% after 2 hours (entry 1). However, when the reaction was carried out

under ball milling for 2 hours, only trace amounts of the target product **3a** were detected regardless of whether agate balls or stainless steel balls were used (entries 2 and 3). Subsequently, we conducted a heating ball milling experiment (entries 4 and 5), which was heated and maintained at 110 °C for 20 minutes. After ball milling for 30 minutes, this process was repeated four times. The results indicated that only trace amounts of **3a** were detected regardless of whether agate balls or stainless steel balls were used. Meanwhile, the yield decreased significantly when the reaction was performed at 110 °C without a solvent, and most of the starting materials

Table 1 Substrate scope of the EMM promoted green synthesis of *tert*-butyl esters under solvent-free conditions^a

$R_1 = \text{Aryl, Alkenyl, alkyl}$ $R_2 = \text{tBu, Me}$

Scope of <i>tert</i> -butyl ester						
 3a, 91%	 3b, 58%	 3c, 78%	 3d, 72%	 3e, 50%	 3f, 60%	 3g, 62%
 3h, 75%	 3i, 49%	 3j, 40%	 3k, 25%	 3l, 71%	 3m, 52%	 3n, 36%
 3o, 83%	 3p, 33%	 3q, 45%	 3r, 52%	 3s, 79%	 3t, 42%	 3u, 88%
 3v, 79%	 3w, 65%	 3x, 52%	 3y, 82%	 3z, 72%	 3aa, 87%	 3ab, 85%
Scope of methyl ester						
 4a, 58%	 4b, 96%	 4c, 40%	 4d, 73%	 4e, 67%	 4f, 86%	
Bioactive compounds						
 3ac: 75%	 3ad: 86%		 3ae: 87%		 3af: 68%	
from Indomethacin	from Ketoprofen		from Oxaprozin		from Februxostat	

^a Conditions: **1**: 0.5 mmol, **2**: 1.0 mmol, high temperature and pressure resistant reaction tube: 10 mL, ferromagnetic rods: SUS304, 5 g, 0.3 × 5.0 mm, reaction time: 2 h, frequency: 50 Hz.

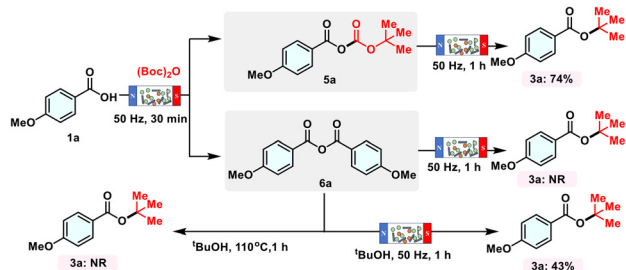
Table 2 Comparison of EMM with solvent-based and ball milling reactions

Entry	Solvent	T/°C	t/h	3a%	5a%	6a%	1a% (recovered)
1 ^a	—	— (EMM)	2	91	Trace	Trace	Trace
2 ^b	—	— (ball milling)	2	Trace	Trace	Trace	92
3 ^c	—	— (ball milling)	2	Trace	Trace	Trace	91
4 ^d	—	110 (ball milling)	2	Trace	35	28	34
5 ^e	—	110 (ball milling)	2	Trace	42	9	45
6 ^f	—	110	2	12	Trace	18	65
7 ^f	—	110	24	18	Trace	27	53
8 ^g	Toluene	110	2	5	43	32	19
9 ^g	Toluene	110	24	14	Trace	52	30

Conditions: **1a**: 0.5 mmol, **2a**: 1.0 mmol, high temperature and pressure resistant reaction tube: 10 mL. ^a Ferromagnetic rods: SUS304, 5 g, 0.3 × 5.0 mm, reaction time: 2 h, frequency: 50 Hz. ^b Agate balls (20 g). ^c Stainless steel balls (20 g). ^d **1a**: 1.0 mmol, **2a**: 2.0 mmol agate balls (20 g), 110 °C, 2 h (heated and maintained at 110 °C for 20 minutes, and then ball milling for 30 minutes; this process has to be repeated four times). ^e **1a**: 1.0 mmol, **2a**: 2.0 mmol stainless steel balls (20 g), 110 °C, 2 h (heated and maintained at 110 °C for 20 minutes, and then ball milling for 30 minutes; this process has to be repeated four times). ^f Oil bath (110 °C). ^g Oil bath (110 °C) solvent: toluene (2 mL).

were recovered (entries 6 and 7) (under EMM conditions, the reaction temperature reached 106 °C; see Fig. 1C). The reaction in toluene proceeded slowly at 110 °C, even after 24 hours, resulting in 14% yield of **3a**. These results indicated that the process of EMM is not only based on collision and the heat generated *via* collision.

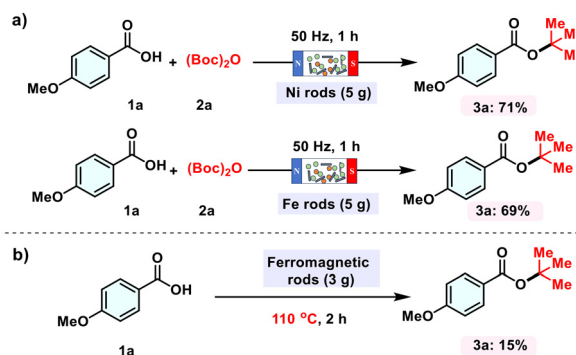
To further explore the reaction process, we conducted several control experiments to examine the intermediates and pathways involved. After 30 minutes of the esterification reaction, we identified and successfully isolated intermediates **5a** and **6a**. It was found that **5a** could directly convert into the target product **3a** with a 74% yield after 1 hour under electromagnetic milling conditions (Scheme 3). In contrast, under the same conditions, **6a** did not produce the target product. However, when 1 mL of *tert*-butanol was added to the reaction system, **3a** was isolated with a 43% yield. Notably, if the reaction was carried out in an oil bath, the addition of *tert*-butanol did not result in the formation of the target product **3a**.



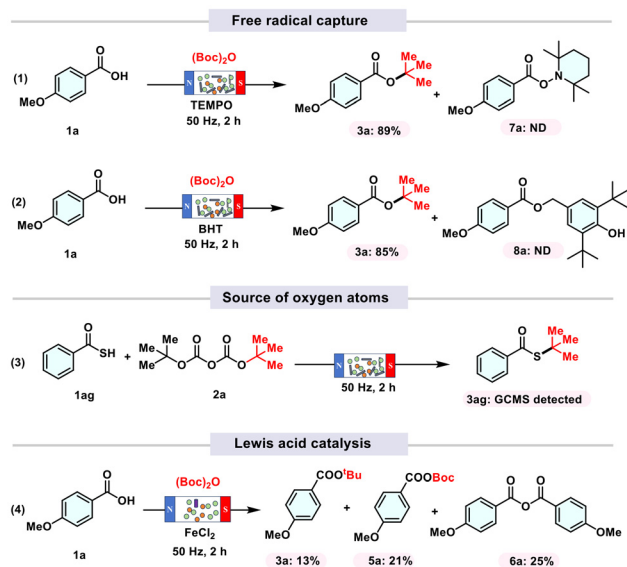
Scheme 3 Control experiment. Conditions: **1a**: 0.5 mmol, **2a**: 1.0 mmol, **5a**: 0.5 mmol, **6a**: 0.5 mmol, high temperature and pressure resistant reaction tube: 10 mL, ferromagnetic rods: SUS304, 5 g, 0.3 × 5.0 mm, reaction time: 2 h, frequency: 50 Hz, *t*-BuOH: 1.0 mL. NR: no reaction.

To investigate whether the metals of the ferromagnetic rods contribute to the formation of the target products, we conducted experiments using pure nickel rods and pure iron rods instead of ferromagnetic ones (Scheme 4a). In both cases, **3a** was obtained in excellent yields. Additionally, under conventional stirring and heating conditions, less than 20% of the target product was produced, regardless of whether ferromagnetic rods were added (Scheme 4b). This suggests that the presence of ferromagnetic rods is not essential for the synthesis of *tert*-butyl esters under electromagnetic milling conditions.

Subsequently, a free radical trapping experiment using TEMPO and BHT was conducted; however, **3a** was obtained in 89% and 85% yields, respectively. However, no TEMPO-trapped products were detected, indicating that it might be not a radical process; however, it could not be excluded either (Scheme 5-1 and 2). Furthermore, we employed thiobenzoic



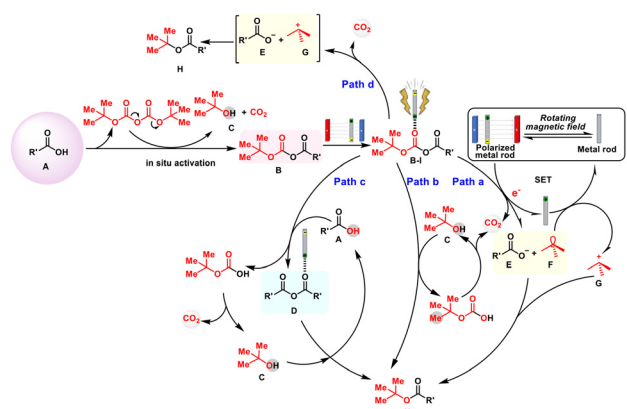
Scheme 4 The influence of metal in steel needles on the experimental results. Conditions: **1a**: 0.5 mmol, **2a**: 1.0 mmol, high temperature and pressure resistant reaction tube: 10 mL, Ni rods, Fe rods: 5 g, 1.0 × 5.0 mm, reaction time: 1 h, frequency: 50 Hz.



Scheme 5 Mechanism exploration experiment. Conditions: **1a**: 0.5 mmol, $(\text{Boc})_2\text{O}$: 1.0 mmol, TEMPO: 1.5 mmol, BHT: 1.5 mmol, FeCl_2 : 20 mmol%, high temperature and pressure resistant reaction tube: 10 mL, ferromagnetic rods: SUS304, 5 g, 0.3×5.0 mm, reaction time: 2 h, frequency: 50 Hz. ND: not detected.

acid **1ag**. After two hours under the standard conditions, the formation of **3ag** was detected *via* GC-MS (see Fig. S8[†]), indicating that the *tert*-butyl group but not *tert*-butyl oxide in the product originates from $(\text{Boc})_2\text{O}$ (Scheme 5-3). Next, Lewis acid FeCl_2 with a stirring bar under EMM conditions was tested, producing the target product **3a** in 13% yield. Although the Lewis acid FeCl_2 could promote the transformation, the low efficiency indicated that Fe^{2+} should not be the catalyst which might get generated during the EMM process (Scheme 5-4).

Herein, four reaction mechanism pathways were proposed (Scheme 6). First of all, the carboxylic acid substance **A** reacts with $(\text{Boc})_2\text{O}$ *in situ* to form the *tert*-butoxycarbonyl intermediate **B**. When exposed to a high-speed rotating magnetic field, the ferromagnetic rod becomes magnetized and charged,



Scheme 6 Possible mechanisms.

which could form a complex **B-I** *via* coordination like the working style of a Lewis acid. In path a, the ferromagnetic rod acts as an electron donor, and facilitates the generation of *tert*-butyl radicals and acyloxy anions *via* single electron transfer. The ferromagnetic rod subsequently acts as an electron acceptor, receiving electrons from the *tert*-butyl radicals to form *tert*-butyl cations. Although no radical adduct was detected, the radical process is still possible.¹³ Finally, the *tert*-butyl cation reacts with an acyloxy anion to form the target *tert*-butyl ester compound **H**. However, the radical capture experiments did not give the desired results. In path b, intermediate **B-I** could react with *tert*-butanol, generated within the system, to yield the target product **H**. Meanwhile, intermediate **D** could be formed through the reaction of the starting material **A** with intermediate **B-I** (path c). Intermediate **D** could further deliver the target product **H** in the presence of *tert*-butanol. However, this transformation could not be realized in a solvent with heating, indicating the key activation role of the ferromagnetic rod. Furthermore, path d is still an alternative pathway. With the activation of the ferromagnetic rod, complex **B-I** dissociates into *tert*-butyl carbocations **G** and **E**, accompanied by the release of CO_2 . Ultimately, the combination of **G** with **E** formed the desired product **H**. Based on the results of Scheme 5-3, path d is the most possible pathway, but we believe paths b and c are also possible. Notably, complex **B-I** serves as a pivotal intermediate across all these pathways, introducing a novel mechanism for bond activation in synthetic chemistry. Its unique ability to facilitate selective bond activation not only expands the toolkit of synthetic chemists, but also paves the way for more efficient and versatile reaction pathways, offering profound implications for the design of new reaction models.

Conclusions

We have developed a novel and efficient method for synthesizing *tert*-butyl esters from carboxylic acids and $(\text{Boc})_2\text{O}$. This solvent-free, base-free, and heating-free approach offers an appealing green and sustainable pathway. The neutral reaction environment is particularly valuable for late-stage modification of sensitive drugs in drug discovery. The reaction is driven by ferromagnetic rods, which become magnetized and charged under a high-speed rotating magnetic field. Based on the control experiments, four potential reaction pathways have been proposed. The coordination between the charged ferromagnetic rods and the reactants plays a crucial role in bond activation during the transformation. Although several key intermediates have been isolated and further transformed into the target molecules, the exact mechanism of bond activation under electromagnetic milling (EMM) conditions remains unclear. Ongoing research in our lab aims to further elucidate this mechanism, with the hope that it will attract broader attention and establish a new field of research.

Author contributions

Yunxia Liu: conceptualization, methodology, data curation, writing – original draft, draft preparation and writing – reviewing and editing. Yan Zhang and Yingyu Qu: data curation; Qing Liu, Fachao Yan and Kai Cao: visualization and investigation; Lizhi Zhang: supervision; and Xinjin Li, Zengdian Zhao and Hui Liu: conceptualization and methodology.

Data availability

The data underlying this study are available in the published article and its ESI.†

Conflicts of interest

There are no conflicts to declare.

Acknowledgements

We gratefully acknowledge the National Natural Science Foundation of China (22078178) and the Youth Innovative Talents Attracting and Cultivating Plan of Colleges and Universities in Shandong Province.

References

- (a) A. Kraft, *Chem. Commun.*, 1996, **1**, 77–79; (b) B. Krebs and H. U. Hürter, *Acta Crystallogr., Sect. A*, 1981, **37**, 163; (c) G. Eulenberger, *Z. Naturforsch., B*, 1981, **36**, 521; (d) G. Solladie, C. Hamdouchi and C. Ziani-Chérif, *Tetrahedron:Asymmetry*, 1991, **2**, 457.
- F. Orvieto, U. Koch, V. G. Matassa and E. Muraglia, *Bioorg. Med. Chem. Lett.*, 2003, **13**, 2745–2748.
- M. Kolb, J. Barth, J. G. Heydt and M. J. Jung, *J. Med. Chem.*, 1987, **30**, 267–272.
- E. Fischer and A. Speier, *Untersuchungen aus Verschiedenen Gebieten: Vorträge und Abhandlungen Allgemeinen Inhalts*, 1924, pp. 285–291.
- S. W. Wright, D. L. Hageman, A. S. Wright and L. D. McClure, *Tetrahedron Lett.*, 1997, **38**, 7345–7348.
- M. T. La and H. K. Kim, *Tetrahedron*, 2018, **74**, 3748–3754.
- Z. Xin, T. M. Gøgsig, A. T. Lindhardt and T. Skrydstrup, *Org. Lett.*, 2012, **14**, 284–287.
- (a) T. W. Greene and P. G. M. Wuts, *Protective Groups in Organic Synthesis*, John Wiley and Sons, New York, 3rd edn 1999; (b) P. J. Kocienski, *Protecting groups*, Georg Thieme, New York, 2000; (c) F. Shirini, M. Mamaghani and S. V. Atghia, *Catal. Commun.*, 2011, **12**, 1088.
- (a) H. Li and J. Balsells, *Tetrahedron Lett.*, 2008, **49**, 2034; (b) J. C. Amedio Jr, G. T. Lee, K. Prasad and O. Repic, *Synth. Commun.*, 1995, **25**, 2599; (c) R. C. Larock, *Comprehensive Organic Transformations*, 1999; (d) E. Ghera and Y. J. Bendavid, *Org. Chem.*, 1988, **53**, 2972; (e) D. Rausch and C. Lambert, *Org. Lett.*, 2006, **8**, 5037; (f) L. D. Bratton, H. Huh and R. A. J. Bartsch, *Chem*, 2000, **37**, 815.
- X. Li, D. Zou, H. Zhu, Y. Wang, J. Li, Y. Wu and Y. Wu, *Org. Lett.*, 2014, **16**, 1836–1839.
- (a) K. K. Kubota, Y. Pang, A. Miura and H. Ito, *Science*, 2019, **366**, 1500–1504; (b) X. Wang, C. Feng, J. Jiang, S. Maeda, K. Kubota and H. Ito, *Nat. Commun.*, 2023, **14**, 5561; (c) K. Kubota, N. Shizukuishi, S. Kubo and H. Ito, *Chem. Lett.*, 2024, **53**, upae056; (d) T. Seo, K. Kubota and H. Ito, *J. Am. Chem. Soc.*, 2023, **145**, 6823–6837.
- (a) S. Pan, F. F. Mulks, P. Wu, K. Rissanen and C. Bolm, *Angew. Chem., Int. Ed.*, 2024, **63**, e202316702; (b) S. Biswas and C. Bolm, *Org. Lett.*, 2024, **26**, 1511–1516; (c) C. Sahu, S. Biswas, R. Hommelsheim and C. Bolm, *RSC Mechanochem.*, 2024, **1**, 38–42; (d) V. S. Pfennig, R. C. Villella, J. Nikodemus and C. Bolm, *Angew. Chem., Int. Ed.*, 2022, **61**, e202116514; (e) F. Puccetti, T. Rinesch, S. Suljić, K. Rahimi, A. Herrmann and C. Bolm, *Chem*, 2023, **9**, 1318–1332.
- (a) R. Hernandez, I. Trakakis, J. Cuccia, T. Friščić and P. Forgione, *Eur. J. Org. Chem.*, 2023, e202300374; (b) M. Pérez-Venegas, T. Friščić and K. Auclair, *ACS Sustainable Chem. Eng.*, 2023, **11**, 9924–9931.
- (a) M. Hribersek, C. Méndez-Gálvez, M. Huber, P. J. Gates, P. Shakari, A. Samanta and L. T. Pilarski, *Green Chem.*, 2023, **25**, 9138–9145; (b) F. J. Ingner, Z. X. Giustra, S. Novosedlik, A. Orthaber, P. J. Gates, C. Dyrager and L. T. Pilarski, *Green Chem.*, 2020, **22**, 5648–5655.
- (a) S. Hutsch, A. Leonard, S. Graetz, M. V. Höfler, T. Gutmann and L. Borchardt, *Angew. Chem., Int. Ed.*, 2024, e202403649; (b) M. Wohlgemuth, S. Schmidt, M. Mayer, W. Pickhardt, S. Graetz and L. Borchardt, *Angew. Chem., Int. Ed.*, 2024, e202405342; (c) H. W. Lee, K. Yoo, L. Borchardt and J. G. Kim, *Green Chem.*, 2024, **26**, 2087–2093.
- C. Patel, E. André-Joyaux, J. A. Leitch, X. Martínez De Irujo-Labalde, F. Ibba, J. Struijs, M. A. Ellwanger, R. Paton, D. L. Browne, G. Pupo, S. Aldridge, M. A. Hayward and V. Gouverneur, *Science*, 2023, **381**, 302–306.
- (a) L. Pontini, J. A. Leitch and D. L. Browne, *Green Chem.*, 2023, **25**, 4319–4325; (b) R. R. Bolt, S. E. Raby-Buck, K. Ingram, J. A. Leitch and D. L. Browne, *Angew. Chem., Int. Ed.*, 2022, **61**, e202210508.
- (a) G.-W. Wang, *Chem. Soc. Rev.*, 2013, **42**, 7668–7700; (b) H. Xu and G.-W. Wang, *J. Org. Chem.*, 2022, **87**, 8480–8491.
- (a) X. Wang, X. Zhang, X. He, G. Guo, Q. Huang, F. You, Q. Wang, R. Qu, F. Zhou and Z. Lian, *Angew. Chem., Int. Ed.*, 2024, **63**, e202410334; (b) F. You, X. Zhang, X. Wang, G. Guo, Q. Wang, H. Song, R. Qu and Z. Lian, *Org. Lett.*, 2024, **26**, 4240–4245; (c) R. Qu, S. Wan, X. Zhang, X. Wang, L. Xue, Q. Wang and Z. Lian, *Angew. Chem., Int. Ed.*, 2024, **63**, e202400645; (d) X. Wang, X. Zhang, L. Xue, Q. Wang, F. You, L. Dai and Z. Lian, *Angew. Chem., Int. Ed.*, 2023, **62**, e202307054.
- (a) Y. Zhao, Z. Yang, X. Wang, Q. Kang, B. Wang, T. Wu, H. Lei, P. Ma, W. Su, S. Wang, Z. Wu, X. Huang, C. Fan and

- X. Wei, *Adv. Sci.*, 2024, **11**, 2404071; (b) S. Chen, C. Fan, Z. Xu, M. Pei, J. Wang, J. Zhang, Y. Zhang, J. Li, J. Lu, C. Peng and X. Wei, *Nat. Commun.*, 2024, **15**, 769.
- 21 (a) J. Zhang, P. Zhang, Y. Ma and M. Szostak, *Org. Lett.*, 2022, **24**, 2338–2343; (b) J. Zhang, P. Zhang, L. Shao, R. Wang, Y. Ma and M. Szostak, *Angew. Chem., Int. Ed.*, 2022, **61**, e202114146.
- 22 (a) K. Xiang, P. Ying, T. Ying, W. Su and J. Yu, *Green Chem.*, 2023, **25**, 2853–2862; (b) P. Ying, J. Yu and W. Su, *Adv. Synth. Catal.*, 2021, **363**, 1246–1271; (c) P. Ying, T. Ying, H. Chen, K. Xiang, W. Su, H. Xie and J. Yu, *Org. Chem. Front.*, 2024, **11**, 127–134; (d) X. Yang, H. Wang, Y. Zhang, W. Su and J. Yu, *Green Chem.*, 2022, **24**, 4557–4565; (e) X. Yang, C. Wu, W. Su and J. Yu, *Eur. J. Org. Chem.*, 2022, e202101440; (f) C. Wu, T. Ying, X. Yang, W. Su, A. V. Dushkin and J. Yu, *Org. Lett.*, 2021, **23**, 6423–6428.
- 23 (a) X. Li, Y. Liu, L. Zhang, Y. Dong, Q. Liu, D. Zhang and H. Liu, *Green Chem.*, 2022, **24**, 6026–6035; (b) Y. Liu, X. Li, Q. Liu, X. Li and H. Liu, *Org. Lett.*, 2022, **24**, 6604–6608; (c) Y. Hou, H. Wang, J. Xi, R. Jiang, L. Zhang, X. Li and H. Liu, *Green Chem.*, 2023, **25**, 2279–2286; (d) Y. Jia, H. Wang, J. Guo, F. Zhang, L. Zhang, X. Li and H. Liu, *J. Org. Chem.*, 2024, **89**, 6704–6713; (e) H. Wang, X. Chi, X. Zhang, L. Zhang, Q. Liu, Z. Zhao and H. Liu, *J. Org. Chem.*, 2024, **89**, 5320–5327.
- 24 (a) S. Styła, *Przegl. Elektrotech.*, 2016, **92**, 103–106; (b) F. S. Bayones, S. M. Abo-Dahab, A. M. Abd-Alla and A. A. Kilany, *Methods Appl. Sci.*, 2021, **44**, 9944–9965; (c) M. Wołosiewicz-Glab, S. Ogonowski and D. Foszcz, *IFAC-PapersOnLine*, 2016, **49**, 67–71; (d) M. Wołosiewicz-Glab, D. Foszcz and S. Ogonowski, *IFAC-PapersOnLine (Elsevier B.V.)*, 2017, **50**, 14964–14969; (e) M. Pawelczyk, Z. Ogonowski, S. Ogonowski, D. Foszcz, D. Saramak, T. Gawenda and D. Krawczykowski, PL4130416, 2015.
- 25 H. Liu, X. Han, X. Feng, L. Zhang, F. Sun, F. Jia, D. Zhang, H. Liu and X. Li, *J. Am. Chem. Soc.*, 2024, **146**, 18143–18150.